

Frequency Domain Packet Scheduling Under Fractional Load for the UTRAN LTE Downlink

A. Pokhariyal[†], G. Monghal[†], K. I. Pedersen[‡], P. E. Mogensen^{†,‡}, I. Z. Kovacs[‡], C. Rosa[‡] and T. E. Kolding[‡]
[†] Aalborg University, [‡] Nokia Networks — Aalborg, Denmark

Abstract—In this paper we investigate the performance of frequency domain packet scheduling (FDPS) under fractional load (FL), based on the UTRAN Long Term Evolution downlink. Under FL, the packet scheduler does not need to transmit on entire system bandwidth due to lack of traffic in the network, which leads to an improvement in the user experienced SINR. System-level simulations show that the proportional fair scheduler tries to optimize resource allocation by avoiding transmission on frequencies that are experiencing severe interference. As an example, FDPS can provide a gain of 4 dB in SINR over the round-robin scheduler, when the load is equal to 25%. The observed interference control is achieved without any centralized management. Further, FDPS under FL can provide an effective trade-off between cell throughput and coverage. The FDPS performance is dependent on the ability of link adaptation to track variations in interference. This ability is reduced when the frequency usage pattern is changing rapidly over time.

I. INTRODUCTION

The downlink radio access of the 3GPP UTRAN long term evolution (LTE) will be based on the orthogonal frequency division multiple access (OFDMA) scheme. The guidelines for the Physical layer design are described in [1]. As LTE supports frequency-domain adaptation techniques in downlink we will investigate the performance of *frequency domain packet scheduling* (FDPS), which refers to fast channel dependent scheduling in both time and frequency domains. Previous FDPS studies [2], [3], [4] indicate that it has significant potential over time-domain only scheduling, e.g. in [4] it is reported that FDPS can provide a gain of around 40% in cell throughput. The main drawbacks of FDPS are high scheduler complexity and increased signaling overhead in the uplink as well as in the downlink. Previous FDPS studies are based on the full load scenario.

As OFDMA can provide intra-cell orthogonality by means of the cyclic prefix, the main source of interference in downlink is *inter-cell interference* (ICI) [5]. It can severely limit the throughput of users near the cell edge, in a reuse 1 network with continuous coverage. When the network is experiencing a lack of traffic, the packet scheduler optimizes resource allocation by transmitting only on a portion of the system bandwidth. This leads to a reduction in ICI and thereby an improvement in SINR, which can be particularly useful to cell-edge users as their data rate can be improved. The focus of this study is the investigation of FDPS under the *fractional load* (FL) scenario.

We assume that there is no co-ordination between the entities responsible for resource allocation in the neighboring cells. The analysis is based on a detailed LTE system-level

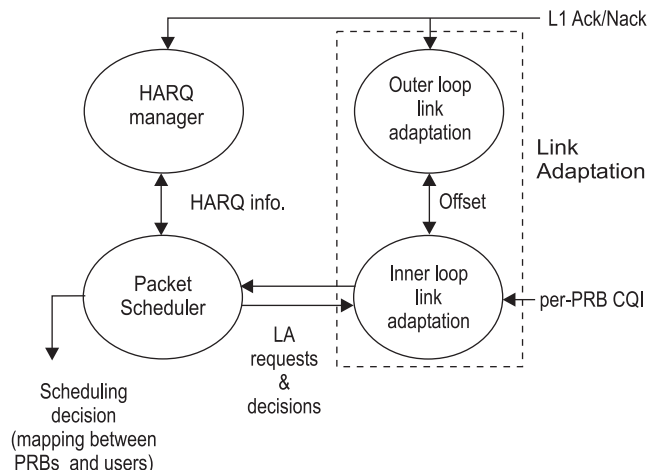


Fig. 1. Interaction between PS, LA, and the HARQ manager entities of the eNode-B that are responsible for dynamic resource allocation.

model, developed according to the guidelines given in [1]. The important scheduling related functions such as link adaptation (LA) and HARQ have been modeled explicitly. Further, as the FDPS performance is sensitive to the accuracy of *channel quality indication* (CQI) reports, realistic assumptions for achievable CQI accuracy and reporting frequency have been used [4].

The paper is organized as follows: Section II describes the interaction between the different functional entities involved in packet scheduling. It also covers the description of the LA functionality and the FDPS algorithm. Section III provides details on the system-model as well as describes the modeling of FL. Section IV covers the results and analysis, while the conclusions are summarized in Section V.

II. PACKET SCHEDULING FRAMEWORK

Fig. 1 illustrates the interaction between the different entities involved in packet scheduling (PS), which are located at the base station (eNode-B) in order to facilitate fast channel dependent scheduling [6]. Following LTE naming convention the basic time-frequency resource available for data transmission is denoted as the physical resource block (PRB). The PRB consists of a fixed number of adjacent OFDM sub-carriers and represents the minimum scheduling resolution in the frequency domain [1]. The PS is the controlling entity in the overall scheduling process. It can consult the LA module to obtain an estimate of the supported data rate for certain users in the cell, for different allocations of PRBs. LA utilizes

frequency-selective CQI feedback from the users, as well as Ack/Nacks from past transmissions, to ensure that the estimate of supported data rate corresponds to a certain BLER target for the first transmissions. Further, outer loop link adaptation has been used to stabilize the BLER performance in the presence of LA uncertainties [7]. It provides a user based adaptive offset on a sub-frame interval that is applied to the received CQI reports. This technique can reduce the impact of biased CQI errors on LA performance [8]. Under FL, the scheduler employs a sub-set of PRBs for transmission. Further, restrictions on the allowed power per active PRB can also be enforced in order to control interference variations in the network. The aim of the scheduler is to optimize the cell throughput for the given load condition under the applied scheduling policy, e.g., proportional fair scheduling in time and frequency [8]. The HARQ manager provides buffer status information as well as transmission format of the pending HARQ retransmissions.

A. Link Adaptation

The experienced SINR of a single radio link is formulated with the aid of Fig. 2. The received SINR measured at the sub-carrier frequency f at scheduling interval n is given by:

$$\text{SINR}(f, n) = \sum_{i=1}^2 \frac{P(f, n) \cdot H_i(f, n)}{N_o(f) + \sum_{k=1}^N I_k(f, n)}, \quad (1)$$

where $P(f, n)$ denotes the transmit power from own cell, $H_i(f, n)$ is the channel power gain experienced at the i th receive antenna, $I_k(f, n)$ denotes inter-cell interference power experienced from surrounding cell k , and N_o represents thermal noise. The expression in (1) is based on a 1x2 MRC receiver. Further, there are $N + 1$ cells in the network. Note that thermal noise is the only time-invariant parameter in (1). Under FL, the PRB containing sub-carrier f can be either in use or inactive in each of the cells. Moreover, the PRB activity state can vary on a sub-frame basis, which results in larger ICI dynamics in comparison with the full load case. At the eNode-B frequency-domain LA is performed by using the knowledge of prevailing channel conditions obtained through frequency selective CQI reports. Due to processing delays at both ends the CQI report measured at the receiver is not available instantaneously at the transmitter, as shown in Fig. 2. If the ICI conditions change before the packet is finally received, LA will not be able to track those changes, leading to a performance deterioration. As a result under FL, the performance of both LA and FDPS becomes sensitive to the time correlation in the PRB "On" and "Off" activity states. In this regard, as the channel fading is correlated in time it is expected that PRB activity states will also be correlated.

B. Frequency Domain Packet Scheduling

We will focus on localized transmissions in the frequency-domain [1]. The overall scheduler is divided into a time-domain (TD) part followed by the frequency-domain (FD) part. The aim of the scheduler is to maximize the utilization of available multi-user diversity in both time and frequency

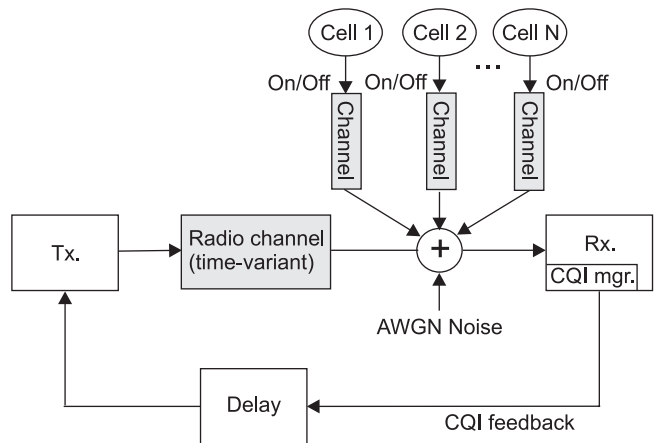


Fig. 2. A single radio link in the reuse 1 LTE downlink, where transmission from neighboring cells leads to ICI. Under FL, the link SINR can vary significantly due to dynamic variations in the ICI.

domains. The details of the scheduler framework as well as its performance evaluation is provided in the related paper [8]. The motivation behind the partitioning of the scheduler is to reduce the complexity of frequency-domain multiplexing algorithm and to handle the restrictions imposed by HARQ retransmissions in an effective manner. A subset of M users are passed to the FD scheduler by the TD scheduler in each sub-frame. Independent scheduling policies can be applied at each scheduler part. The task of the TD scheduler is to achieve inter-user fairness, while the FD scheduler tries to optimize the spectrum efficiency. The choice of M depends on the scheduler complexity as well as on the allowed DL control overhead. Control signaling is required to notify users of incoming transmissions, and the resulting overhead depends on M . The default scheduler is based on the well known *proportional-fair* (PF) metric, which is applied in both time and frequency. Further, the reference scheduler consists of round-robin scheduling in frequency, while the TD scheduler is based on the PF metric.

III. SYSTEM MODEL

The performance evaluation is based on a detailed system-level model of LTE, following the guidelines in [1]. The system bandwidth is fixed at 10 MHz, and the Physical layer settings are based on the LTE working assumptions. The main simulation parameters are listed in Table I, assuming the macro-cell case 1 deployment scenario. We assume that the PRB bandwidth is equal to 375 kHz, resulting in 24 PRBs. Scheduling related functions are explicitly modeled in the three center cells only. The remaining fifty-four cells act as a source of ICI. The link-to-system level mapping is based on the *exponential effective SNR metric* (EESM) model [8]. The location of users is randomly assigned with a uniform distribution within each of the three center cells. It is assumed that the distance dependent path loss and shadow fading is constant during a packet call. A finite buffer best effort traffic model is employed, where each user downloads a 2 Mbit packet. As soon as the download is completed, the session

TABLE I
DEFAULT SIMULATION PARAMETERS [1].

| Parameter | Setting |
|--------------------------------------|---|
| System bandwidth | 10 MHz |
| Sub-carriers per PRB | 25 |
| Cellular Layout | Hexagonal grid, 19 cell sites, 3 cells per site |
| Inter-site distance | 500 m |
| Total eNode-B transmit power | 46 dBm |
| Penetration loss | 20 dB |
| Shadowing standard deviation | 8 dB |
| Max. users multiplexed per sub-frame | 6 |
| Power per active PRB, P_{PRB} | 32.2 dBm |
| C | 20 sub-frames |
| Traffic model | Single 2 Mbit packet |
| Power delay profile | ITU Typical Urban, 20 paths |
| Ack/Nack delay | 2 ms |
| CQI log-normal error std. | 1 dB |
| CQI reporting resolution | 1 dB |
| CQI delay | 4 ms |
| Pilot, control channel overhead | 28.5% (2/7 symbols) |
| Modulation/code rate settings | QPSK (R= 1/3, 1/2, 2/3), 16QAM (R=1/2, 2/3, 4/5), 64QAM (R=1/2, 2/3, 4/5) |
| HARQ model | Ideal chase comb. |
| No. of HARQ processes | 6 |
| 1st Tx. BLER target | 20% |
| UE speed | 3 km/h |
| UE receiver | 1x2 MRC |
| Channel estimation | Ideal |
| Cell selection margin | 2 dB |

is terminated and a new call is immediately started at a new random location. The serving cell is selected randomly among the strongest cells within a selection margin of 2 dB. The key performance indicators are the average cell throughput, user throughput distribution and coverage at 5% outage.

A. Modeling of Fractional Load

As scheduling is not explicitly simulated in the non-center cells a model is required for FL scenario. We have selected the well-known discrete two-state homogenous Markov-chain based stochastic model, as shown in Fig. 3. The states represent whether a PRB is "On" or "Off". The parameters of the Markov model can be tuned to provide a certain average rate of state transitions. This facilitates the modeling of a

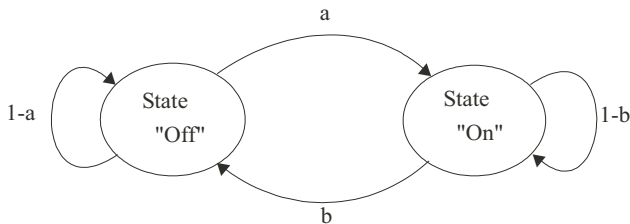


Fig. 3. Discrete two-state homogeneous Markov chain used for modeling of FL.

TABLE II
FRACTIONAL LOAD SCENARIOS INVESTIGATED.

| Load factor, P_1 | Number of active users per cell, L | Avg. num of active PRBs, \bar{X} |
|--------------------|--------------------------------------|------------------------------------|
| 0.25 | 5 | 6 |
| 0.50 | 10 | 12 |
| 0.75 | 15 | 18 |
| 1.00 | 20 | 24 |

dynamic FL scenario with known correlation behavior between PRB activity states. Independent Markov chains are used in all the interfering cells in the network, assuming the same state transition probabilities. The activity state of each PRB is updated every 0.5 ms.

Let P_1 denote the probability that a PRB is "On", while $P_0 = 1 - P_1$ denotes the probability that it is "Off". Given the Markov chain in Fig. 3, we can express the state probabilities for PRB "Off" and "On" states as,

$$P_0 = \frac{b}{a+b} \quad (2)$$

$$P_1 = \frac{a}{a+b} \quad (3)$$

Given this simple stochastic model for controlling the On/Off activity for each of the M PRBs in each of the interfering cells, there will be X active PRBs for a given cell in a sub-frame, such that $X \in [0, 1, 2, \dots, M]$. The probability of experiencing q consecutive "On" states is geometrically distributed with a mean value given by:

$$C = \frac{1}{b} \quad (4)$$

From (3) and (4) and since a and b should be in the range $[0, 1]$, parameter C is subject to the following constraint,

$$C > \max \left\{ 1, \frac{P_1}{1-P_1} \right\} \quad (5)$$

The value of C relative to the CQI delay determines how effectively LA can track the SINR variations. We select $C = 20$ sub-frames by default, such that it is much larger than the CQI delay (8 sub-frames). In the center cells, the number of active PRBs is determined by using a Binomial distribution based on the given load factor, P_1 . By default constant power allocation in frequency is considered, i.e., fixed power per active PRB denoted by P_{PRB} . We also show performance results for the flexible power allocation scheme, where the total power is divided equally among the active PRBs, for comparison purposes. We investigate FDPS performance under different load conditions enumerated in Table II. The ratio of average number of active PRBs to the number of users L , i.e., \bar{X}/L , is kept constant, in order to make a fair comparison.

IV. SIMULATION RESULTS

Fig. 4 shows the probability distribution function (PDF) of the number of active PRBs for different FL scenarios listed

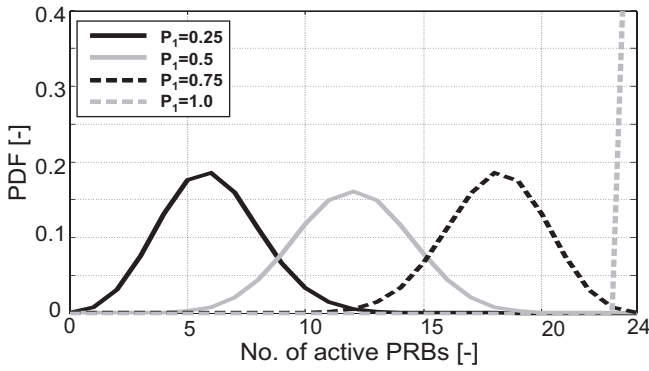


Fig. 4. Statistics for availability of PRBs collected from entire network.

in Table II. The statistics are collected from all the cells in the network. The PDF curves follow expected trends with the mean value of active PRBs in each case matching with \bar{X} in Table II.

Fig. 5 illustrates the behavior of key parameters that affect system performance. The results in Fig. 5 (a) confirm that FL results in an improvement in the sub-carrier SINR. Further, a significant gain of FDPS (PF) over reference scheduler is seen especially at low load, e.g., at $P_1 = 0.25$ the SINR improvement with reference scheduler is 6 dB (not shown here), while it is 10 dB with FDPS. The additional gain is attributed to the use of CQI, which lowers the probability of scheduling on the same PRBs in neighboring cells. The interference control seen here is achieved without relying on any centralized management. Fig. 5 (b) illustrates the cumulative density function (CDF) of the total transmit power used at each scheduling node. The curves follow expected trends as the eNode-B tunes the transmit power according to P_1 . Fig. 5 (c) depicts the CDF of the experienced SINR measured on a packet basis. We observe a higher gain in SINR than expected at low load, similar to Fig. 5 (a). The CDF curves of Fig. 5 (d) illustrate that LA is able to map the improvement in SINR due to FL into a gain in user throughput, especially at the tail of the throughput distribution, i.e., in terms of coverage. However, the curves converge at the top, which is a result of the limited MCS range, e.g., the highest available MCS, 64QAM 4/5, is selected at around 15 dB, while the SINR can increase up to 40 dB.

Fig. 6 illustrates the performance of FDPS in terms of average cell throughput and coverage, which is defined as the data rate at 5% outage. It is observed that FDPS can provide a trade-off between cell throughput and coverage, e.g., when $P_1 = 0.25$, the coverage is improved by a factor of around two, while the average cell throughput is halved, in comparison with the full load case. We compare the results obtained with the following Shannon Theorem based approximation,

$$\text{cell_throughput} \cong W \cdot P_1 \cdot \log_2 \left(1 + \text{SINR} \cdot \frac{1}{P_1} \right), \quad (6)$$

where W denotes the bandwidth. P_1 appears twice in (6) to represent the FL induced bandwidth reduction as well as the SINR improvement from the reduction in ICI. By substituting

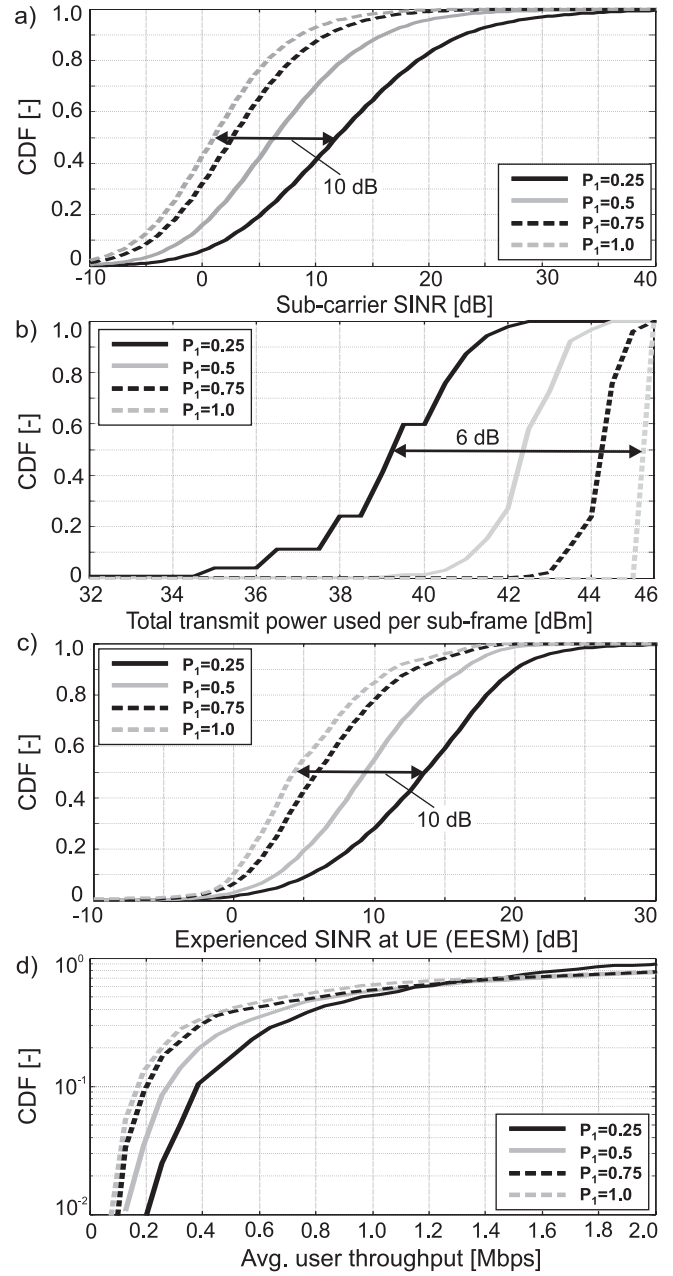


Fig. 5. Behavior of key parameters governing system performance.

the median value of SINR (~ 1 dB) from Fig. 5 (a) and the cell throughput from Fig. 6 (a) for the $P_1 = 1.0$ case into (6) we obtain the Shannon based estimate of the cell throughput for the different cases, also shown in Fig. 6 (a). It can be seen that there is a good match between the estimated and the observed cell throughput values, except for the $P_1 = 0.25$ case. In the latter scenario, due to the limited MCS range LA is not able to map the very high SINR values into corresponding value of throughput. Further, compared to the reference scheduler PF scheduling in frequency can provide an additional gain of 10-15% in throughput and coverage.

Fig. 7 (a) and Fig. 7 (b) illustrate the impact of rate of change

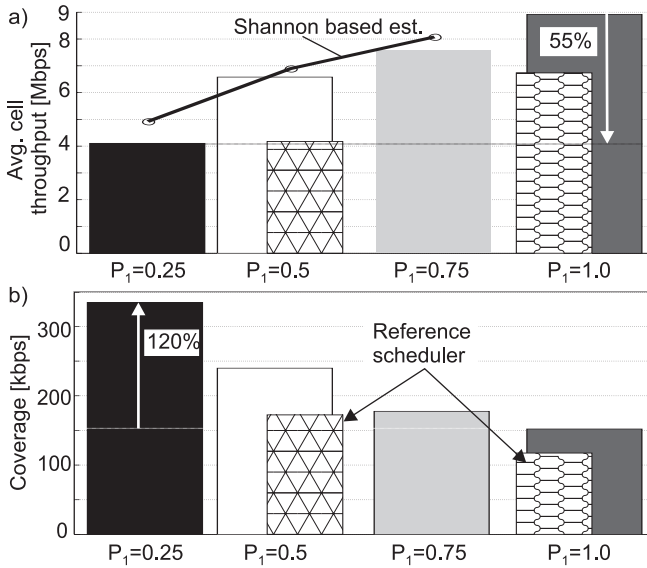


Fig. 6. Average cell throughput and coverage performance as a function of P_1 . The results for the reference scheduler are shown for two FL cases.

of the PRB allocation pattern. Frequent changes in the PRB activity results in a performance loss, due to the inability of LA to track the ICI variations. The impact is significant at low load, e.g., a loss of up to 25% in coverage is seen in Fig. 7 (b).

Fig. 8 illustrates the comparative performance of the constant and the flexible power allocation schemes. The two schemes have quite similar performance as the deployment scenario is mainly interference limited, and the use of higher transmit power does not lead to a similar SINR improvement.

V. CONCLUSIONS

In this paper we have investigated the performance of frequency domain packet scheduling (FDPS) under fractional load (FL) scenario, based on the UTRAN Long Term Evolution downlink. Under FL, the packet scheduler does not need to allocate entire system bandwidth for transmission, due to lack of traffic in the network, which leads to an improvement in the experienced SINR. System-level simulations show that the proportional fair scheduler tries to optimize resource allocation by avoiding transmission on frequencies that are experiencing severe interference. As an example, FDPS can provide a gain of 4 dB in SINR over the frequency-blind scheduler, when the load is equal to 25%. The observed interference control is achieved without relying on any centralized management. Further, FDPS under FL can provide an effective trade-off between cell throughput and coverage, e.g., when the load is 25%, coverage is improved by a factor of two, while cell throughput is halved compared to full load case. The FDPS gain depends on the ability of link adaptation to track the variations in interference. This ability is reduced if the frequency usage pattern is changing at a fast rate.

REFERENCES

[1] 3GPP Technical Report 25.814, version 7.1.0, *Physical Layer Aspects for Evolved UTRA*, September 2006.

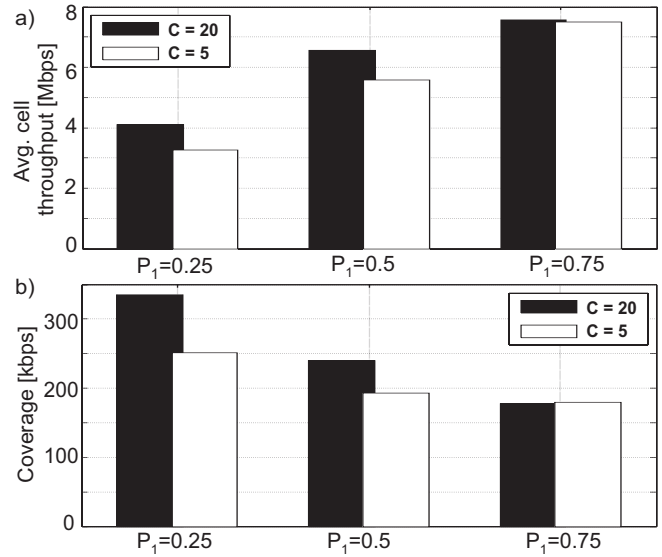


Fig. 7. Impact of the PRB switching rate on FDPS performance.

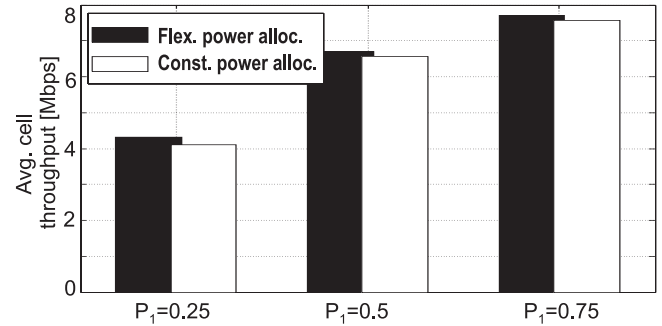


Fig. 8. Potential of adaptive power allocation with FDPS, $C = 20$.

[2] B. Classon, P. Sartori, V. Nangia, X. Zhuang, and K. Baum, "Multi-dimensional Adaptation and Multi-user Scheduling Techniques for Wireless OFDM systems," in *IEEE ICC International Conference on Communications*, vol. 3, Orlando, Florida, USA, May 2003, pp. 2251–2255.

[3] S. Nagata, Y. Ofuji, K. Higuchi, and M. Sawahashi, "Optimum Resource Block Bandwidth for Frequency Domain Channel-Dependent Scheduling in Evolved UTRA Downlink OFDM Radio Access," in *Proceedings of IEEE Vehicular Technology Conference (VTC)*, Melbourne, Australia, May 2006.

[4] A. Pokhariyal, T. E. Kolding, and P. E. Mogensen, "Performance of Downlink Frequency Domain Packet Scheduling for the UTRAN Long Term Evolution," in *Proceedings of IEEE Personal Indoor and Mobile Radio Communications Conference (PIMRC)*, Helsinki, Finland, September 2006.

[5] Texas Instruments, "Performance of Inter-Cell Interference Mitigation with Semi-Static Frequency Planning for EUTRA Downlink," *3GPP TSG-RAN1, R1-060368*, February 2006.

[6] H. Holma and A. Toskala, Eds., *HSDPA/HSUPA for UMTS – High Speed Radio Access for Mobile Communications*. John Wiley & Sons Ltd, 2006.

[7] M. Nakamura, Y. Awad, and S. Vadgama, "Adaptive Control of Link Adaptation for High Speed Downlink Packet Access (HSDPA) in W-CDMA," in *Proceedings of Wireless Personal Multimedia Communications Conference (WPMC)*, vol. 2, Honolulu, Hawaii, October 2002, pp. 382–386.

[8] A. Pokhariyal, K. I. Pedersen, G. Monghal, I. Z. Kovacs, C. Rosa, T. E. Kolding, and P. E. Mogensen, "HARQ Aware Frequency Domain Packet Scheduler with Different Degrees of Fairness for the UTRAN Long Term Evolution," in *Proceedings of the IEEE Vehicular Technology Conference (VTC)*, Dublin, Ireland, April 2007.